J. Phys. D: Appl. Phys. **29** (1996) 2297–2303. Printed in the UK

Magnetorheological fluid composites

J Popplewell† and R E Rosensweig

Exxon Research and Engineering Company, 1545 Route 22 East, Annandale, NJ 08801-3059, USA

Received 23 January 1996

Abstract. An interesting extension in the use of magnetic fluids has resulted from the development of magnetic fluid composites obtained by dispersing micrometre-sized non-magnetic particles in a magnetic fluid. The composites possess a yield stress in a magnetic field which can be described at sufficiently high strain rates by the Bingham relation $\tau = \tau_y + \eta_0\dot{\gamma}$, where τ is the shear stress perpendicular to the applied field, τ_y the extrapolated yield stress, $\dot{\gamma}$ the strain rate and η_0 the plastic viscosity. Thus, a composite, particle concentration $\phi = 0.35$, in a field 0.036 T with $\bar{\chi} = 0.96$ has a yield stress τ_y of 26 Pa. The yield stresses obtained experimentally for different ϕ and B_0 correspond well to values predicted theoretically by Rosensweig using a determination of τ_y based on a continuum concept of unsymmetric stress that develops in the deformed but unyielded anisotropic medium.

1. Introduction

A magnetic fluid composite is a dispersion of micrometre-sized non-magnetic particles in a magnetic fluid carrier. The magnetic fluid itself is typically a colloidal suspension of magnetite (Fe_3O_4) particles of 100 Å diameter which are, therefore, 10^9 times smaller in volume than the non-magnetic particles of the composite. Thus, the composite can for most purposes be regarded as a dispersion of non-magnetic particles in a homogeneous magnetic medium. The magnetic properties of the composite result entirely from the magnetic fluid carrier which is a superparamagnetic fluid with a saturation magnetization some 10% that of bulk magnetite. The rheological and magnetic properties of magnetic fluids which determine the properties of the composites have been intensively studied and reviewed by Rosensweig [1].

The initial studies of composites were undertaken by Skjeltorp [2], who studied films containing a monolayer of polystyrene spheres of diameter $D = 10$ μm. The films were marginally thicker than the sphere diameter, thus allowing free movement of the particles in two dimensions. The particles can be considered to form voids in the magnetic fluid which acquire an induced moment when a magnetic field is applied, opposite to the direction of the field. This induced moment $\boldsymbol{m}$ can be written to a first approximation in terms of an effective fluid susceptibility χ_{eff} and in the case of a linear medium

$$\boldsymbol{m}(\theta) = \mu_0\chi_{eff}(\theta)v\boldsymbol{H}(\theta) \tag{1}$$

where μ_0 is the permeability of free space, v is the particle volume, $\boldsymbol{H}$ the field applied and θ the field direction. In determining χ_{eff} the particle and sample shape have to be taken into account. It is shown in the appendix that

$$\chi_{eff}(\theta) = \frac{-[1 + N_p(\theta)]\chi_f}{(1 + \chi_f)[1 + N_s(\theta)\chi_f]} \tag{2}$$

where χ_f is the fluid susceptibility and $N_s(\theta)$ and $N_p(\theta)$ are de-magnetizing factors for sample and particle, respectively.

The dipole interaction energy between two identical spherical particles separated by a distance d is given by

$$U = \frac{1}{4\pi\mu_0}m^2(\theta)\frac{(1 - 3\cos^2\theta)}{d^3} \tag{3}$$

where θ is the angle between the field and the line of centres of the two particles. The energy is a minimum and attractive when $\theta = 0$ and the particles are in contact with $d = D$, the particle diameter. It then follows that

$$U = -\frac{m^2}{2\pi\mu_0 D^3} \tag{4}$$

where m is given by (1) and χ_{eff} by (2). The particles will attract one another to form chains in the field direction, however, only if the coupling constant λ representing the ratio of the dipole–dipole energy to thermal energy is greater than unity, that is

$$\lambda = \frac{m^2}{4\pi\mu_0 D^3 kT} = \frac{mM}{24kT} > 1 \tag{5}$$

where $m = \mu_0 M v$ and $\mu_0 M$ is the magnetic moment per unit volume.

The number of particles n in a chain has been derived theoretically by de Gennes and Pincus [3] and Gast and Zukowski [4] who showed that

$$n = \left[1 - \frac{2}{3}\left(\frac{\phi}{\lambda^2}\right)e^{2\lambda}\right]^{-1} \tag{6}$$

† Present address: School of Electronic Engineering and Computer systems, University of Wales, Bangor, Gwynedd LL57 1UT, UK.

0022-3727/96/092297+07$19.50

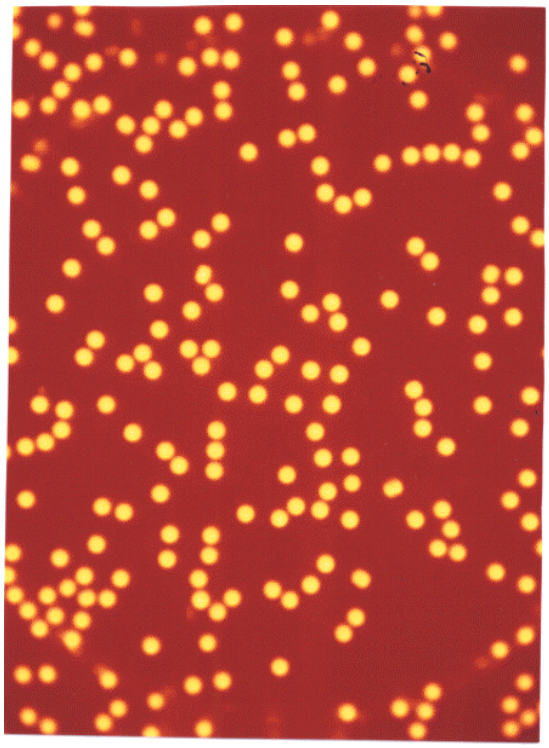

Figure 1. A composite containing polystyrene spheres, D = 10 μm, in an isopar M-based magnetic fluid $\mu_0 M_s$ = 0.035 T, B_0 = 0.

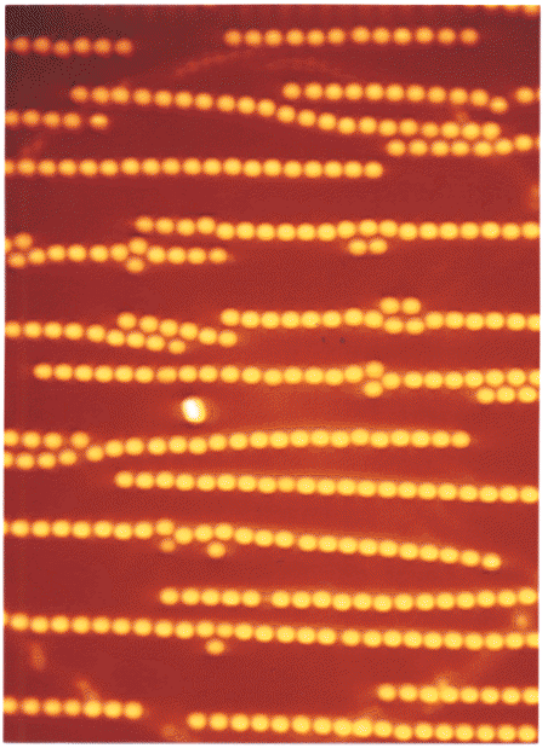

Figure 2. The same composite as in figure 1 with a field B_0 = 0.02 T applied in the chain direction.

where λ is given by (5) and ϕ is the volumetric concentration. Thus, the chain length becomes infinite at a critical concentration

$$\phi_c = \frac{3}{2}\left(\frac{\lambda^2}{e^{2\lambda}}\right). \tag{7}$$

In such cases, when $\phi = \phi_c$, the chains provide a continuous path across the sample, aligning parallel to the field. The structures formed in a monolayer composite film as studied by Skjeltorp [2] are shown in figures 1 and 2. The composite contains uniform polystyrene particles, $D = 10$ μm, dispersed in an isopar M-based magnetic fluid with $\mu_0 M_s = 0.035$ T. The field applied in plane in the chain direction in figure 2 is 0.02 T. Figures 3 and 4 show samples containing hollow glass spheres with a distribution of particle sizes, median diameter 8 μm. The chain structure is less regular when a field 0.02 T is applied, with a thickening or coarsening of the chain structure at high particle concentrations as shown in figure 5.

The structures observed in figure 5 are similar to those found in electrorheological fluids and magnetorheological fluids consisting of ferromagnetic particles dispersed in a non-magnetic carrier. The particle interactions in the latter would always be stronger than those in magnetic fluid composites of the same particle concentration and particle size because the particle moments are an order of magnitude greater and it would be expected, that these would make more effective magnetorheological fluids. However, the magnetic fluid composites are more versatile. The particles

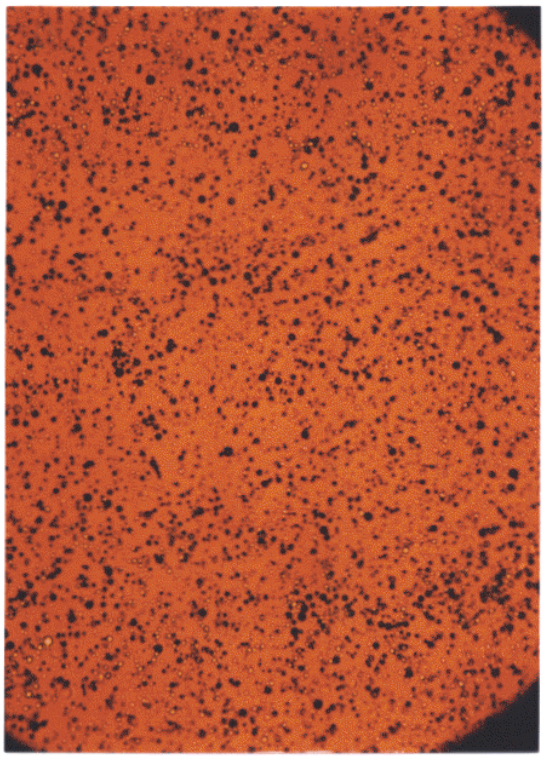

Figure 3. A composite containing a distribution of hollow glass spheres, mean diameter D = 8 μm, in a hydrocarbon magnetic fluid $\mu_0 M_s$ = 0.015 T, $\phi \simeq 0.1$ and B_0 = 0.

can be chosen from a wide selection of non-magnetic

Figure 4. The same composite as shown in figure 3 but with a field B_0 = 0.02 T applied in the chain direction.

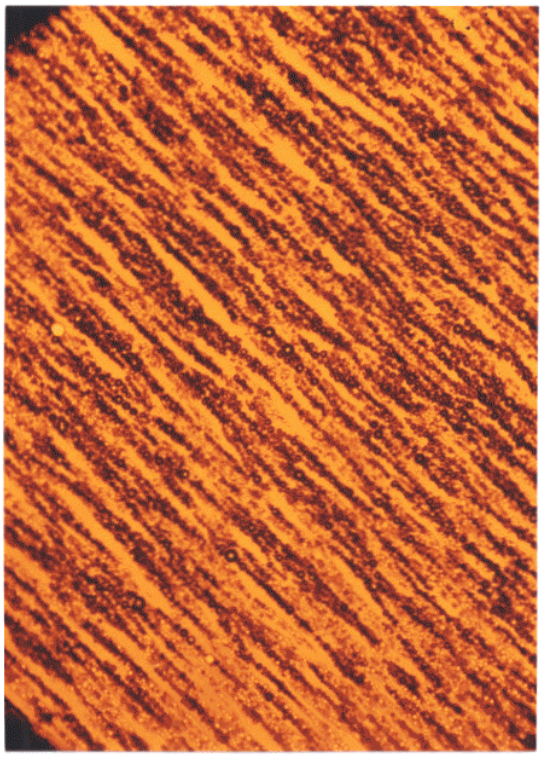

Figure 5. A composite containing a distribution of hollow glass spheres, mean diameter D = 8 μm, in a hydrocarbon magnetic fluid $\mu_0 M_s$ = 0.015 T and $\phi \simeq 0.3$. The field B_0 = 0.02 T is applied in the chain direction.

materials covering a range of densities which can be matched to that of the magnetic fluid. Moreover, since the induced moment is determined by the superparamagnetic carrier, the particle moment disappears in zero field in contrast to the case for ferromagnetic particles and aggregation in zero field is inhibited. Finally, since the choice of particle material is so extensive, either metallic or non-metallic particles can be used, providing the composite with a rich variety of electrical and dielectric properties.

Magnetorheological fluids can be used in similar situations to those of electrorheological fluids, that is in computer-controlled hydraulic systems for vehicles, field-controlled damping devices, magnetic valves and so on. The control is through magnetic fields derived from low-voltage sources rather than electric fields requiring high voltages of 10^3–10^4 V mm^{-1}.

Initial studies on magnetorheological fluid composites were undertaken by Kashevskii *et al* [5] who studied the effects of magnetic fields on the viscosity of composites containing non-magnetic particles of different shapes, concluding that plate-like particles produce a greater magnetorheological response than do spherical particles. They did not, however, discuss the factors which determine yield stress values. These were studied by Bossis and Lemaire [6], who considered in detail the yield stress values of composites in a magnetic field and obtained yield stress values for composites containing both magnetic and non-magnetic particles.

2. Theory

Rosensweig [7] developed a continuum model of a composite based on a laminar layer structure with magnetic elements aligned in the field direction, to determine theoretical expressions for the yield stress. It was proposed that, when a shear stress is applied perpendicular to the field direction, the layer structure distorts as shown in figure 6. χ_1 denotes the isotropic susceptibility of medium 1 and χ_2 that of medium 2. H_0 is the applied field and $\mu_0 M$ the magnetization of the magnetic layer. The inclination of the layer, α, increases as the stress τ increases until, at the yield point τ_y, $\alpha = \pi/4$ for a layer with no de-magnetization. For a system with de-magnetization α depends on the susceptibility but is close to $\pi/4$ with $\chi_1 < 2$. The cone and plate viscometer where aluminium is used as the cone and plate material corresponds to a system with de-magnetization. In this case, if the cone angle is small and the separation between cone and plate small compared to the diameter, the yield stress is given approximately [7] by

$$\tau_y = \frac{\mu_0 H_0^2 \phi(1-\phi)\bar{\chi}^2}{4\{(1+\bar{\chi})(1+\phi\bar{\chi})[1+\bar{\chi}(1-\phi)]\}^{1/2}} \qquad (8)$$

with de-magnetizing factors taken as appropriate to those of a thin film, that is $D = 1$ in the direction of $\boldsymbol{H}_0$ and 0 perpendicular to $\boldsymbol{H}_0$. When the cone and plate are made from iron and the thickness is small (8) would still be a reasonable approximation for the yield stress. $\bar{\chi}$ is the chord susceptibility with $\bar{\chi} = \chi_f(H_0 \cos\alpha)$ rather

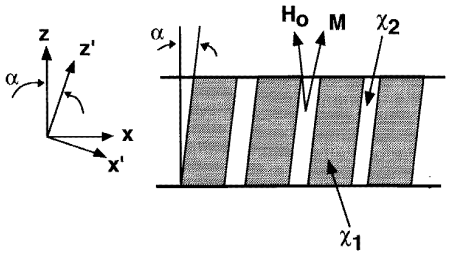

Figure 6. The laminar model of a composite proposed by Rosensweig [7]. The shaded region represents the magnetic component and the unshaded region the non-magnetic component. Unprimed axes indicate laboratory coordinates. Primed axes represent principal axes of the sheared composite.

Table 1. The susceptibility χ_f for the kerosene-based magnetic fluid carrier, $\mu_0 M_s$ = 0.045 T.

$\chi_f = M/H$	1.87	1.81	1.47	1.08	0.85	0.73
B_0 T (10^{-4})	0	50	100	200	300	400

than $\chi_f(H_0)$ with α approximated to $\pi/4$ to represent the susceptibility along the principal axis of the deformed sample of figure 4 more realistically.

3. Experimental

Composites were prepared by dispersing hollow glass beads, mean diameter 8 ± 2 μm, in a kerosene-based magnetic fluid with saturation magnetization $\mu_0 M_s = 0.045$ T and viscosity 7 cP. The hollow glass beads, supplied by Potters Industries, Inc, had a density of 1.1×10^3 kg m^{-3} which matched that of the carrier magnetic fluid. Thus, effects of gravitation in determining the rheological properties of the composites could be discounted. The coupling coefficient λ given by (5) is of the order of 10^5 in a field of 10^{-2} T so that substantial particle chaining would be expected. Typical structures are shown in figures 4 and 5. The carrier magnetic fluid had susceptibility $\chi_f = M/H$ as shown in table 1.

Rheological studies were performed at 24 °C with a cone-and-plate viscometer that allows the applied stress to be independently controlled. The plate diameter was 25 mm and the cone angle 0.1 rad. The cone material was chosen to be either aluminium or iron and the surface roughness measured with a profilometer was 10 μm. A magnetic field was applied perpendicular to the shear plane by means of a pair of coils surrounding the cone and plate. The magnitude of the field could be varied in the range 0–0.036 T when the aluminium cone and plate were used and in the range 0–0.140 T when the cone and plate were iron. Radial field gradients in the horizontal plane acted to restrain the composite to the gap between the cone and plane and counteracted dynamic effects resulting from the cone rotation. Gradients in the vertical plane were small by comparison.

4. Results

The variation in strain rate with stress was measured at different fields for composites with particle concentrations $\phi = 0.15, 0.18, 0.23, 0.31$ and 0.35. The maximum stress applied was 80 Pa and strain rates up to 300 s^{-1} were observed. Examples of the stress against strain rate variations, measured in a fixed field, are shown in figures 7–11 for $\phi = 0.15, 0.18, 0.23, 0.31$ and 0.35. There are two quite distinct regions in these curves. At high strain rates, the strain rate variation with stress is linear, following a Bingham relationship:

$$\tau = \tau_y + \dot{\gamma}\eta_0 \tag{9}$$

where τ_y is the yield stress, $\dot{\gamma}$ the strain rate and η_0 the plastic viscosity which can be approximated to the zero field viscosity. For composites for which the Bingham relationship applies, the yield stress can be obtained by extrapolation to zero shear rate. Equation (9) does not apply, however, when the strain rate is small and the relationship between stress and strain rate is complex. It is possible that slippage occurs between the cone or plate surfaces and the solid composite when the applied stress is below the yield stress value. Bossis and Lemaire [6] mentioned the importance of surface roughness in determining yield stress values. Studies of the surface roughness of the cone and plate indicate that, on a microscopic scale, the surfaces are far from smooth (as compared, for example, to glass) but slippage might well result from weak bonding between the particle chains of the composite and the rheometer cone and plate. Popplewell *et al* [8] showed that, when an iron cone and plate are used and a field is applied, the extra adhesion of the chains due to image forces restricts slippage, giving a higher actual yield stress and lower strain rates than those for the aluminium equivalent in the same field. This is illustrated in figure 12. In addition to the effects of slippage, the chains would fracture at weak points at a stress below the yield stress value expected for perfectly structured chains of spherical particles. The nonlinear behaviour at low strain rates was also observed by Keshevskii *et al* [5], Klingenberg and Zukowski [9] and Gast *et al* [4] in electrorheological fluids. In [9, 10] the nonlinear behaviour at low stresses was attributed to fracture of the solidified electrorheological fluid, which spreads as the strain rate increases until the particles are all dispersed. The yield stresses obtained experimentally from the Bingham relationship (9) are shown for different values of ϕ and field $B_0 = \mu_0 H_0$ in table 2.

The agreement between the theoretical values for the yield stress calculated from (8) and the experimental values is remarkably good at all concentrations and fields, indicating that the continuum model of Rosensweig [7] is appropriate for these composite systems. A comparison between the variation of the normalized yield stress with ϕ and $\bar{\chi}$ obtained experimentally with that predicted by the theory of Rosensweig (8) is given in figure 13. Again excellent agreement between theory and experiment is observed.

Table 2. A comparison between experimental and theoretical values of the yield stress τ_y for a composite containing hollow glass beads in a magnetic fluid with $\mu_0 M_s$ = 0.045 T.

	τ_y (B_0 = 0.036 T)		τ_y (B_0 = 0.024 T)	
ϕ	Experimental (Pa±20%)	Theoretical (Pa)	Experimental (Pa±20%)	Theoretical (Pa)
0.15	16	15.0	10	7.5
0.18	19	17.6	9	10.9
0.23	21	20.8	14	12.8
0.31	23	24.8	15	15.3
0.35	26	26.3	16	16.1

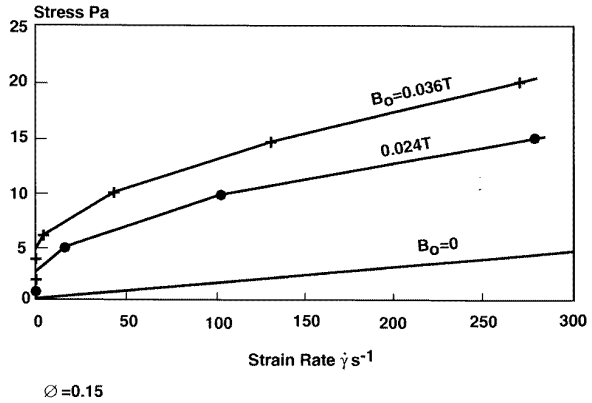

Figure 7. The stress against strain rate variation for a composite containing hollow glass beads, D = 8 μm, with concentration ϕ = 0.15 and field B_0 = 0.036 and 0.024 T. η_0 = 15 cP.

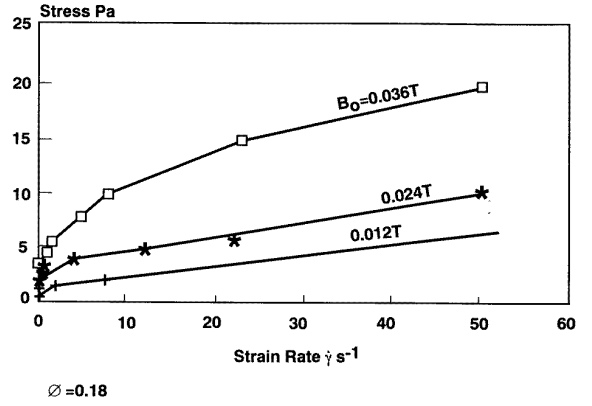

Figure 8. The stress against strain rate variation at low strain rates for a composite containing hollow glass beads, D = 8 μm, with concentration ϕ = 0.18 and field B_0 = 0.006, 0.012 and 0.024 T. η_0 = 16 cP.

The variation of stress with strain rate with increasing applied stress can be different from that observed with decreasing stress. This apparent hysteresis is, however, a time-dependent phenomenon, as shown in figure 14. It is reasonable to expect the strain rate to increase progressively as chains, formed in the field, disperse with time and conversely the strain rate decreases as chains develop. It is important, therefore, to allow 20 min between measurements to ensure steady state conditions.

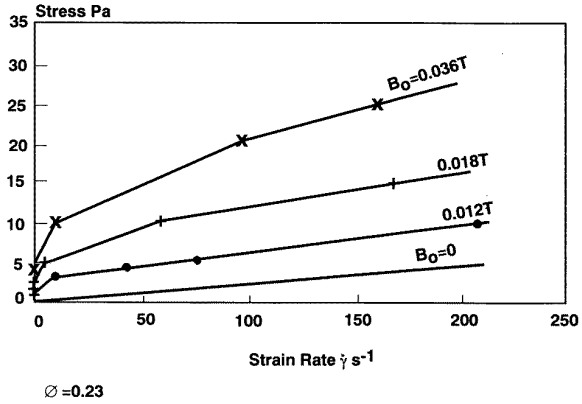

Figure 9. The stress against strain rate variation for a composite containing hollow glass beads, D = 8 μm, with concentration ϕ = 0.23 and field B_0 = 0.012, 0.018 and 0.036 T. η_0 = 22 cP.

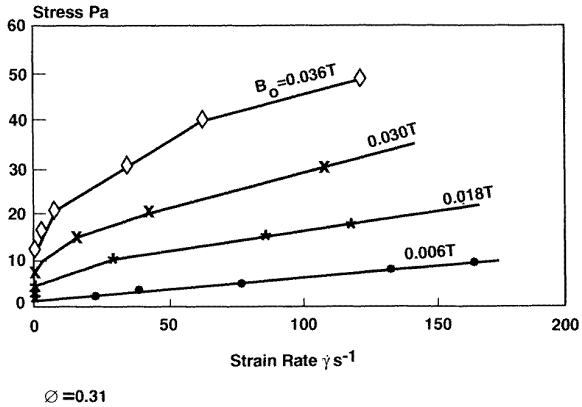

Figure 10. The stress against strain rate variation for a composite containing hollow glass beads, D = 8 μm, with concentration ϕ = 0.31 and field B_0 = 0.006, 0.018, 0.030 and 0.036 T. η_0 = 62 cP.

5. Summary

The magnetorheological properties of composites at low stresses and strain rates are difficult to interpret and are probably very structure-sensitive. Measurements may also depend on whether the surfaces of the viscometer cone and plate are rough or smooth or whether they are made of non-ferrous or ferrous material.

At high stress and strain rates a Bingham relationship

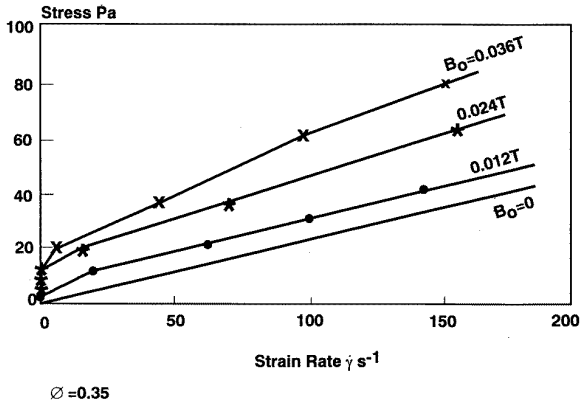

Figure 11. The stress against strain rate variation for a composite containing hollow glass beads, D = 8 μm, with concentration ϕ = 0.35 and field B_0 = 0.024 and 0.036 T. η_0 = 250 cP.

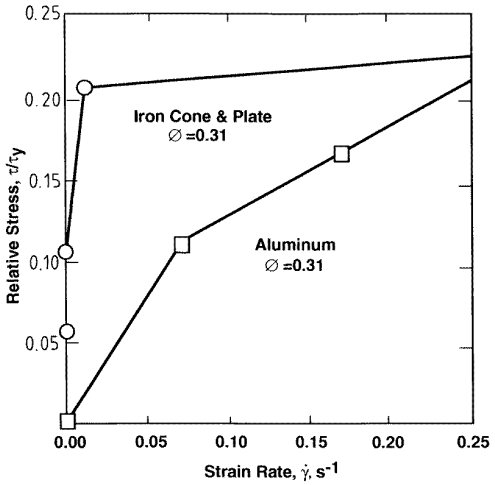

Figure 12. The strain rate variation with applied stress, indicating the possibility of slippage at the walls of the aluminium cone and plate with B_0 = 0.024 T (for aluminium) and 0.028 T (for iron).

allows a yield stress to be determined which matches with theory (7). The values of yield stress measured are similar to those obtained by Bossis and Lemaire [6] but are still some 10^3 times smaller than the best values obtained from electrorheological fluids. Higher values could be obtained by using needle or plate-like particles to increase the packing fraction, as shown by Kashevskii *et al* [5], or by increasing the magnetic fluid magnetization and the field applied. Although yield stress values are below those obtained from many electrorheological fluids or magnetorheological fluids containing magnetic particles, composites based on magnetic fluids are a suitable and possibly better alternative when yield stress values are less important (as in damping applications) than having well-defined and reproducible rheological properties coupled with product reliability.

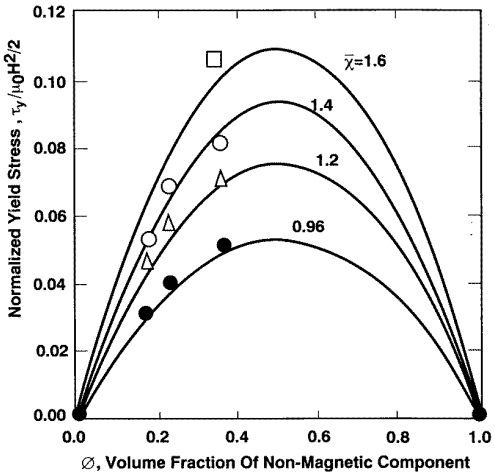

Figure 13. Theoretical predictions of yield stress given by (8) compared with experimental values.

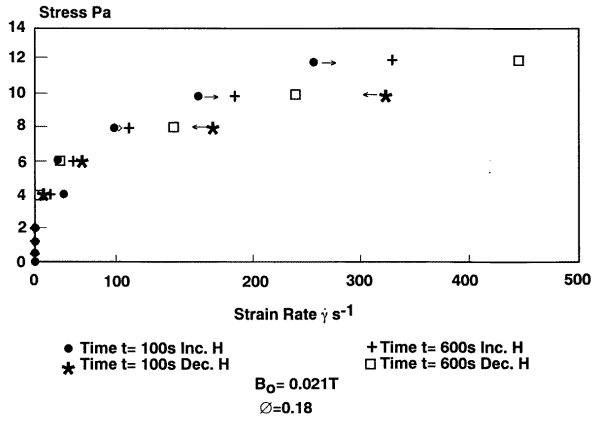

Figure 14. The variation of strain rate with applied stress showing how the strain rate varies over a 600 s interval. Measurements are taken both in increasing and in decreasing stress modes, B_0 = 0.012 T and ϕ = 0.18.

Acknowledgments

The authors would like to record their appreciation of the help given by J Siller in preparing samples and assisting with viscosity measurements. The technical support at the School of Engineering and Computer Systems, University of Wales, Bangor is also duly acknowledged.

Appendix. The effective particle susceptibility χ_{eff}

The effective susceptibility of a non-magnetic particle immersed in a magnetic fluid was given by Skjeltorp [2] as

$$\chi_{eff} = \frac{\chi_f}{[1 + (N_s - N_p)]\chi_f} \qquad \text{(A1)}$$

where χ_f is the magnetic fluid susceptibility and N_s and N_p are the respective de-magnetizing factors for the sample and particle. The solution (A1), however, is physically

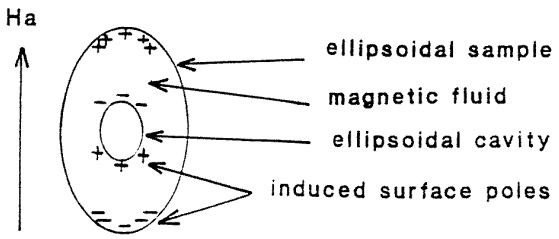

Figure 15. The pole distribution on cavity and sample surfaces in the field H_a.

unacceptable since χ_{eff} can change sign and take positive values when χ_f is large and $N_p > N_s$. it is clear from physical consideration of the total field distribution that the particle susceptibility must always be negative (diamagnetic). The following analysis is believed to give an exact expression for χ_{eff}.

With reference to figure 15, H_a is the field applied along the axis for an ellipsoidal magnetic fluid sample containing an ellipsoidal cavity. The poles induced by H_a are shown in figure 15, giving an induced diamagnetic moment to the cavity which, in the case of a composite, would be a non-magnetic particle of volume v. Let H_f be the field in the magnetic fluid in the absence of the cavity and M_f the corresponding fluid magnetization. It should be noted that the magnetization of the fluid with the cavity present is not uniform and at the cavity surface has values M'_f in field H'_f.

Thus, in the absence of the cavity

$$H_f = H_a - N_s M_f \tag{A2}$$

$$M_f = \chi_f H_f. \tag{A3}$$

From (A2) and (A3) it follows that

$$M_f = \frac{\chi_f}{1 + \chi_f N_s} H_a. \tag{A4}$$

When the size of the cavity is much smaller than the system as a whole the field inside the cavity is

$$H_c = H_f + N_p M_f. \tag{A5}$$

Thus, substituting for H_f from (A2) and for M_f from (A4), we have

$$H_c = \frac{1 + \chi_f N_p}{1 + \chi_f N_s} H_a. \tag{A6}$$

Invoking the continuity of the induction field $\boldsymbol{B}$ across the cavity interface on the centre-line gives

$$B_c = \mu_0 H_c = \mu_0 (H'_f + M'_f) \tag{A7}$$

and, from (A3),

$$M'_f = \chi_f H'_f. \tag{A8}$$

Thus, eliminating H'_f between (A8) and (A9),

$$M'_f = \frac{\chi_f}{1 + \chi_f} H_c. \tag{A9}$$

Writing the definition of the effective susceptibility

$$\chi_{eff} = -\frac{M'_f}{H_a} \tag{A10}$$

gives

$$\chi_{eff} = -\frac{\chi_f (1 + N_p \chi_f)}{(1 + \chi_f)(1 + N_s \chi_f)} \tag{A11}$$

which is substantially different from the Skjeltorp expression (A1). The field H_c in the cavity and H_f in the sample without the cavity are both rigorously uniform but H'_f and M'_f are spatially variable over the cavity interface. χ_{eff} is the susceptibility of an isolated particle of the same size and shape as that of the cavity and yielding the same distribution of poles when subjected to the applied field H_a. The susceptibility is diamagnetic and the induced moment of the particle is opposite to the direction of the field, as shown in figure 15.

References

[1] Rosensweig R E 1985 *Ferrohydrodynamics* (Cambridge: Cambridge University Press)
[2] Skjeltorp A T 1983 *Phys. Rev. Lett.* **51** 2306; 1985 *J. Appl. Phys.* **57** 3285
[3] de Gennes P G and Pincus P 1970 *Phys. Kondens. Mater.* **11** 189
[4] Gast A P and Zukowski C F 1989 *Adv. Colloid Interface Sci.* **30** 153
[5] Kashevskii B E, Kordonskii V I and Prokhorov I V 1988 *Magnetohydrodynamics* vol 3 (New York: Plenum) p 368
[6] Bossis G and Lemaire E 1991 *J. Rheol.* **35** 1345; Lemaire E and Bossis G 1991 *J. Phys. D: Appl. Phys.* **24** 1473
[7] Rosensweig R E 1995 *J. Rheol.* **39** 179
[8] Popplewell J, Rosensweig R E and Siller J K 1995 *J. Magn. Magn. Mater.* **149** 53
[9] Klingenberg D J and Zukoski C F 1990 *Langmuir* **6** 15